Fairbanks, G., Steck, T. L., & Wallach, D. F. H. (1971) *Biochemistry 10*, 2606.
Frey, P. A., & Abeles, R. H. (1966) *J. Biol. Chem. 241*, 2732.
Honda, S., Toraya, T., & Fukui, S. (1980) *J. Bacteriol. 143*, 1458.
Hunkapiller, M. W., & Hood, L. E. (1978) *Biochemistry 17*, 2124.
Hunkapiller, M. W., & Hood, L. E. (1980) *Science (Washington, D.C.) 207*, 523.
Jacobs, E. E., & Sandai, O. R. (1960) *J. Biol. Chem. 235*, 231.
Jacobs, E. E., Andrews, E. C., Cunningham, W., & Crane, F. L. (1966) *Biochem. Biophys. Res. Commun. 25*, 87.
Johnson, N. D., Hunkapiller, M. W., & Hood, L. E. (1979) *Anal. Biochem. 100*, 335.
Kaplan, B. H., & Stadtman, E. R. (1968) *J. Biol. Chem. 243*, 1794.
Laemmli, U. K. (1970) *Nature (London) 227*, 680.
Lee, H. A., & Abeles, R. H. (1962) *J. Biol. Chem. 236*, 2347.
Lowry, O. H., Rosebrough, N. J., Farr, A. L., & Randall, R. J. (1951) *J. Biol. Chem. 193*, 265.
MacLennon, D. H., & Tzagoloff, A. (1968) *Biochemistry 7*, 1603.
Matsubara, H. (1970) *Methods Enzymol. 19*, 642.
Moore, K. W., Bachovchin, W. W., Gunter, J. B., & Richards, J. H. (1979) *Biochemistry 18*, 2776.
Ne'eman, Z., Kahane, I., Karvartovsky, J., & Razin, S. (1972) *Biochim. Biophys. Acta 266*, 255.
Panefsky, H. S., & Tzagoloff, A. (1971) *Methods Enzymol. 22*, 204.
Poznanskaya, A. A., Tanizawa, K., Soda, K., Toraya, T., & Fukui, S. (1977) *Bioorg. Khim. 3*, 111.
Poznanskaya, A. A., Tanizawa, K., Soda, K., Toraya, T., & Fukui, S. (1979) *Arch. Biochem. Biophys. 194*, 379.
Retey, J., Umani-Ronchi, A., Seibl, J., & Arigoni, D. (1966) *Experientia 22*, 502.
Singer, S. J. (1971) *Structure and Function of Biological Membranes* (Rothfield, L. I., Ed.) pp 145–222, Academic Press, New York.
Tanford, C., & Reynolds, J. A. (1976) *Biochim. Biophys. Acta 457*, 133.
Toraya, T., Uesaka, M., & Fukui, S. (1974) *Biochemistry 13*, 3895.
Toraya, T., Shirakashi, T., Kosoga, T., & Fukui, S. (1976) *Biochem. Biophys. Res. Commun. 69*, 745.
Vanderkooi, G. (1974) *Biochim. Biophys. Acta 344*, 307.
Zagalak, B., Frey, P. A., Karabatsos, G. L., & Abeles, R. H. (1966) *J. Biol. Chem. 241*, 3028.

Synthesis and Characterization of a New Fluorogenic Active-Site Titrant of Serine Proteases†

D. Campbell Livingston, John R. Brocklehurst, John F. Cannon,‡ Steven P. Leytus, John A. Wehrly,§ Stuart W. Peltz, Gary A. Peltz,⊥ and Walter F. Mangel*

ABSTRACT: The molecule 3′,6′-bis(4-guanidinobenzoyloxy)-5-[*N*′-(4-carboxyphenyl)thioureido]spiro[isobenzofuran-1-(3*H*),9′-[9*H*]xanthen]-3-one, abbreviated FDE, was designed and synthesized as a fluorogenic active-site titrant for serine proteases. It is an analogue of *p*-nitrophenyl *p*-guanidinobenzoate (NPGB) in which a fluorescein derivative is substituted for *p*-nitrophenol. FDE and NPGB exhibit similar kinetic characteristics in an active-site titration of trypsin in phosphate-buffered saline, pH 7.2. The rate of acylation with FDE is extremely fast (k_2 = 1.05 s^{-1}) and the rate of deacylation extremely slow (k_3 = 1.66 × 10^{-5} s^{-1}). The K_s is 3.06 × 10^{-6} M, and the $K_{m(app)}$ is 4.85 × 10^{-11} M. With two of the serine proteases involved in fibrinolysis, the rate of acylation with FDE is also fast, k_2 = 0.112 s^{-1} for urokinase and 0.799 s^{-1} for plasmin, and the rate of deacylation is slow, k_3 = 3.64 × 10^{-4} s^{-1} for urokinase and 6.27 × 10^{-6} s^{-1} for plasmin. The solubility limit of FDE in phosphate-buffered saline is 1.3 × 10^{-5} M, and the first-order rate constant for spontaneous hydrolysis is 5.1 × 10^{-6} s^{-1}. The major difference between FDE and NPGB is the detectability of the product in an active-site titration. *p*-Nitrophenol can be detected at concentrations no lower than 10^{-6} M whereas fluorescein can be detected at concentrations as low as 10^{-12} M. Thus, FDE should be useful in quantitatively assaying serine proteases at very low concentrations.

The role of proteolytic enzymes in a wide variety of biological processes is being increasingly recognized (Reich et al., 1975). Proteolysis is involved in the temporal and spatial control of enzyme function, metabolic and secretory pathways, morphogenesis, and cell surface interactions. Proteases are intimately involved not only in such processes as blood coagulation, fibrinolysis, and digestion but also in ovulation (Beers et al., 1975), cell migration (Ossowski et al., 1973a,b, 1975), tumorigenicity (Unkeless et al., 1973; Ossowski et al., 1973a,b; Pollack et al., 1974; Christman et al., 1975; Jones et al., 1975), embryogenesis (Strickland et al., 1976), recombination and derepression (Miskin & Reich, 1980), etc. For many proteins, proteolysis occurs at an early step in their synthesis, is required for activation of enzymatic activity, and is the final step leading to their destruction. The discovery of additional roles for proteases in biological processes is, in part, dependent upon the availability of more sensitive and quantitative assays.

† From the Imperial Cancer Research Fund, Lincoln's Inn Fields, London WC2A 3PX, England (D.C.L.), Standard Telecommunication Laboratories, Ltd., Harlow, Essex, England (J.R.B.), and the Department of Biochemistry, University of Illinois, Urbana, Illinois 61801 (J.F.C., S.P.L., J.A.W., S.W.P., G.A.P., and W.F.M.). *Received November 24, 1980.* This investigation was supported by Grant CA 25633 from the National Institutes of Health and by a Biomedical Research Support Grant from the University of Illinois.

‡ Present address: Department of Biochemistry, University of Wisconsin, Madison, WI 53706.
§ Present address: E. I. du Pont de Nemours & Co., Inc., Experimental Station, Wilmington, DE 19898.
⊥ Present address: Stanford University School of Medicine, Stanford, CA 94305.

0006-2960/81/0420-4298$01.25/0

Active-site titrants are extremely useful reagents for accurately determining the molar concentration of active enzyme molecules. A large number of variables involved in rate assays that limit their accuracy can be avoided in active-site titrations (Bender et al., 1966; Chase & Shaw, 1969). Rate assays require the use of enzyme units which, although reflective of enzymatic activity, are not necessarily indicative of the absolute or molar concentration of enzyme. Compared to rate assays, active-site titrations are much easier to perform and interpret. Furthermore, in active-site titrations, the absolute standard is usually an easily purified small molecule rather than a "pure" enzyme and substrate, the standards in rate assays.

Active-site titrants are especially useful in assaying proteases. These enzymes hydrolyze themselves at rates which are concentration dependent. Thus, good active-site titrants are those which react quickly with the enzyme, resulting in the formation of an enzymatically inactive, stable acyl-enzyme intermediate and the release of a product that can be detected at low concentrations. *p*-Nitrophenyl *p*-guanidinobenzoate, hereafter abbreviated NPGB,[1] is an excellent active-site titrant of many serine proteases (Chase & Shaw, 1967, 1969). In the presence of NPGB, trypsin is rapidly acylated and *p*-nitrophenol released. The acyl-enzyme intermediate, *p*-guanidiniobenzoyl-trypsin, is stable, exhibiting a half-time for deacylation of 12 h. NPGB is sufficiently soluble to be used at concentrations much greater than the $K_{m(app)}$. Furthermore, NPGB is relatively stable in aqueous buffers. These and other characteristics of NPGB fulfill most of the criteria of an ideal active-site titrant, except one. The major problem lies in the detectability of the product of the reaction, *p*-nitrophenol. The lowest concentration of *p*-nitrophenol that can be measured with an accuracy of better than 2% is 10^{-6} M.

Here we describe the synthesis and initial characterization of a new active-site titrant of the esterase activity of serine proteases—3′,6′-bis(4-guanidinobenzoyloxy)-5-[*N*′-(4-carboxyphenyl)thioureido]spiro[isobenzofuran-1(3*H*),9′-[9*H*]xanthen]-3-one (FDE). It is an analogue of NPGB in which a fluorescein derivative is substituted for *p*-nitrophenol. It is similar to NPGB in that it exhibits the same excellent kinetic characteristics in an active-site titration of trypsin. It is different from NPGB in that by substituting chromophores, the detectability of the product in an active-site titration is increased 6 orders of magnitude. This increase in sensitivity has allowed us to assay some serine proteases under conditions heretofore not possible (Leytus et al., 1981; Liu et al., 1980).

Materials and Methods

Materials. NPGB was purchased from ICN and dissolved in redistilled dimethylformamide. Benzamidine hydrochloride hydrate was purchased from Aldrich. Stock solutions were prepared in phosphate-buffered saline. Fluorescein isothiocyanate (isomer I), *p*-aminobenzoic acid, and dicyclohexylcarbodiimide were purchased from Sigma. Thin-layer chromatography was performed on Kieselgel 60 F_{254} (Merck) by using a solvent system of 3% methanol in wet diethyl ether. Bovine pancreas trypsin, 3 times crystallized, was purchased from Worthington. Stock solutions were prepared in 1 mM HCl and stored at −20 °C. An active-site titration with NPGB indicated 74% of the total protein (determined by absorbance) was active trypsin. The trypsin concentrations reported here are active-site concentrations. Reference standard human urokinase was purchased from Leo Pharmaceuticals. Stock solutions were prepared in phosphate-buffered saline at pH 7.2 and stored at −20 °C. Lysine–Sepharose 4B and cyanogen bromide activated Sepharose 4B were purchased from Pharmacia. Phosphate-buffered saline contained 0.137 M NaCl, 2.68 mM KCl, 8.08 mM Na_2HPO_4, 1.47 mM KH_2PO_4, 0.91 mM $CaCl_2$, and 0.49 mM $MgCl_2$ at pH 7.2.

Fluorescence and Absorbance Measurements. Active-site titrations using FDE and NPGB were performed in phosphate-buffered saline, pH 7.2. FDE titrations were monitored with a Perkin-Elmer MPF 44-A fluorescence spectrophotometer containing a Universal Digital Readout meter connected to a Hewlett-Packard Model 7015 X-Y recorder with time base. The excitation and emission wavelengths were 491 and 514 nm, respectively. The bandwidth of both monochromators was 4 nm. The fluorescence spectrophotometer was standardized by using a poly(methacrylate) block embedded with rhodamine B so that the relative fluorescence was comparable in different experiments. NPGB titrations were monitored at 400 nm in a Beckman Acta cIII spectrophotometer with a time chart recorder.

Determination of the FDE Concentration. Stock solutions of FDE in redistilled dimethylformamide were routinely prepared at concentrations as high as 20 mM and are stable in the dark at 4 °C for at least 1 month. The concentration of a stock solution was determined by first incubating an equal volume of FDE with 1 N NaOH for 2 h at room temperature. That solution was then diluted 100-fold with water before measuring the absorbance. The molar extinction coefficient is 77 800 at 491 nm in 0.01 N NaOH. This was determined by weighing crystals of 5-[*N*′-(4-carboxyphenyl)thioureido]-3′,6′-dihydroxyspiro[isobenzofuran-1(3*H*),9′-[9*H*]-xanthen]-3-one, dissolving them in 0.01 N NaOH, and determining the absorbance at 491 nm.

Analysis of Titration Curves. The kinetic parameters of each titration curve were determined with a Hewlett-Packard Model 9825A computer interfaced to a Model 9864A digitizer board and 9872 plotter. The kinetic profile of a titration curve was traced with the digitizer and recorded into computer memory. The computer then calculated the *y* axis intercept of the extrapolated steady-state line, *B*, and the slope of the steady-state line, *A*. The first-order rate constant, *b*, was then obtained by a computer-performed least-squares treatment of the equation $\ln (Be^{-bt}/B) = -bt$. The analysis was visually confirmed by having the computer direct the plotter to graph the digitized titration curve, the extrapolated steady-state line, and a plot of $-\ln (Be^{-bt}/B)$ vs. time.

Fluorescence Lifetimes and Quantum Yields. Fluorescence lifetimes were measured on a cross-correlation, phase/modulation fluorometer (Spencer & Weber, 1969) with improved electronics from SLM Instruments, Inc., Urbana, IL. The excitation light was modulated at a frequency of 18 MHz. The excitation wavelength was 480 nm. Emission was observed through a Corning 3-69 cutoff filter. Fluorescence quantum yields were determined relative to a quantum yield of 0.92 for fluorescein (Seybold et al., 1969; Weber & Teale, 1957) by the method of Parker & Rees (1960). Spectra were recorded on a ratiometric spectrofluorometer equipped with digital electronics (Wehrly et al., 1976; Jameson et al., 1977). The instrument utilized a Hamamatsu R928 photomultiplier tube which, with its extended S-20 response, made unnecessary the correction of the emission spectra for the determination of

[1] Abbreviations used: FDE, 3′,6′-bis(4-guanidinobenzoyloxy)-5-[*N*′-(4-carboxyphenyl)thiouredio]spiro[isobenzofuran-1(3*H*),9′-[9*H*]-xanthen-3-one; FME, 5-[*N*′-(4-carboxyphenyl)thioureido]-3′-(4-guanidinobenzoyloxy)-6′-hydroxyspiro[isobenzofuran-1(3*H*),9′-[9*H*]-xanthen]-3-one; FUE, 5-[*N*′-(4-carboxyphenyl)thioureido]-3′,6′-dihydroxyspiro[isobenzofuran-1(3*H*),9′-[9*H*]xanthen]-3-one; NPGB, *p*-nitrophenyl *p*-guanidinobenzoate.

relative quantum yields (Wehrly, 1979). The excitation wavelength was 491 nm, and the emission was scanned from 480 to 620 nm. A 2-nm bandwidth was used on both the excitation and emission monochromators. Total spectra areas were used for the determination of the relative quantum yields.

Preparation of Dog Plasmin. Dog plasmin was prepared by activating plasminogen with urokinase coupled to Sepharose beads (Castellino & Sodetz, 1976). Coupling was accomplished by dissolving 6600 Plough units of human urokinase in 1 mL of coupling buffer (0.1 M $NaHCO_3$ and 0.5 M NaCl, pH 8.3) and adding that solution to a 1-mL suspension containing 0.28 g of cyanogen bromide activated Sepharose 4B in coupling buffer. The suspension was continuously mixed by inversion for 2 h at room temperature. The beads were then washed with several volumes of coupling buffer followed by treatment with 1 M ethanolamine, pH 8.0, to block any remaining active groups. Adsorbed protein was removed by a series of four cycles of high pH (coupling buffer) and low pH (0.1 M sodium acetate and 0.5 M NaCl, pH 4) washes. The beads were then suspended in coupling buffer and stored in 50% glycerol at 4 °C. Dog plasminogen was converted to plasmin by adding 0.5 mL of plasminogen (1–10 mg/mL) dissolved in phosphate-buffered saline containing 0.1 M lysine to 0.5 mL of urokinase–Sepharose 4B washed with phosphate-buffered saline. After continuous mixing by inversion for 45 min at room temperature, the beads were removed by centrifugation. The plasmin in the supernatant was stored in 25% glycerol at −20 °C. Dog plasminogen was purified by the procedure described in Leytus et al. (1981).

Conversion of Relative Fluorescence Units to the Concentration of Active Sites. The standard curve relating fluorescence to the concentration of active sites was obtained as follows. One-milliliter solutions of FDE (4.40×10^{-7} M) in phosphate-buffered saline were incubated with trypsin or plasmin at concentrations ranging from 1.11×10^{-8} M to 6.59×10^{-8} M. The protease concentrations were dilutions of stock solutions whose molar concentrations were determined by NPGB active-site titrations. The magnitude of the fluorescence burst minus the magnitude of the fluorescence of a similar solution not containing enzyme is defined as ΔF. A graph of ΔF vs. the protease concentration yields a straight line intersecting the origin. The slope of this line was used to convert ΔF to the molar concentration of active sites.

Results

Design of FDE. The molecule 3′,6′-bis(4-guanidinobenzoyloxy)-5-[*N*′-(4-carboxyphenyl)thioureido]spiro[isobenzofuran-1(3*H*),9′-[9*H*]xanthen]-3-one (FDE, fluorescein diester) was designed as a fluorogenic active-site titrant of serine proteases (Figure 1a). It is an analogue of NPGB in which a fluorescein derivative is substituted for *p*-nitrophenol. FDE is nonfluorescent because the fluorescein moiety is in the lactone state. In the presence of a serine protease, however, one of the guanidinobenzoyl esters is hydrolyzed, yielding 5-[*N*′-(4-carboxyphenyl)thioureido]-3′-(4-guanidinobenzoyloxy)-6′-hydroxyspiro[isobenzofuran-1(3*H*),9′-[9*H*]xanthen]-3-one [FME, fluorescein monoester (Figure 1b)]. FME should be highly fluorescent, because the fluorescein moiety is in the quinone state. By substitution of chromophores, the detectability of the product in an active-site titration can be increased 6 orders of magnitude, from 10^{-6} M for *p*-nitrophenol to 10^{-12} M for fluorescein. Since FDE is an ester of guanidinobenzoate, as is NPGB, the kinetic properties exhibited in an active-site titration of serine proteases should be similar to those exhibited by NPGB. Specifically, these properties include (1) a rapid rate of acylation, (2) a slow rate of deacylation, (3) a $K_{m(app)}$ far below the solubility limit of the substrate, and (4) a slow rate of spontaneous hydrolysis in aqueous solutions.

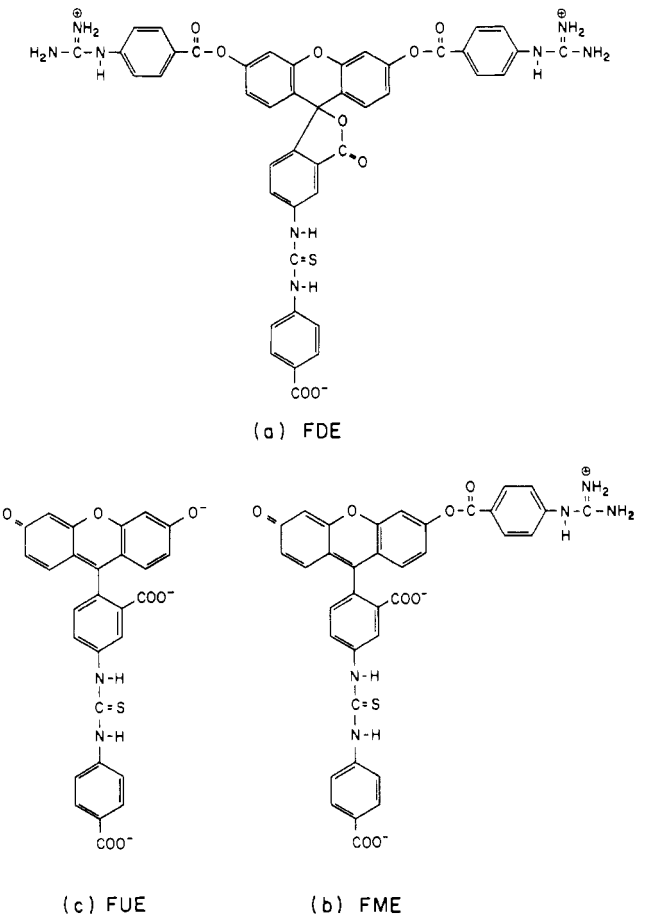

FIGURE 1: Structures of (a) FDE, (b) FME, and (c) FUE in phosphate-buffered saline at pH 7.2: (a) 3′,6′-bis(4-guanidinobenzoyloxy)-5-[*N*′-(4-carboxyphenyl)thioureido]spiro[isobenzofuran-1(3*H*),9′-[9*H*]xanthen]-3-one; (b) 5-[*N*′-(4-carboxyphenyl)thioureido]-3′-(4-guanidinobenzoyloxy)-6′-hydroxyspiro[isobenzofuran-1(3*H*),9′-[9*H*]xanthen]-3-one; (c) 5-[*N*′-(4-carboxyphenyl)thioureido]-3′,6′-dihydroxyspiro[isobenzofuran-1(3*H*),9′-[9*H*]-xanthen]-3-one.

Synthesis of FDE. 5-[*N*′-(4-Carboxyphenyl)thioureido]-3′,6′-dihydroxyspiro[isobenzofuran-1(3*H*),9′-[9*H*]xanthen]-3-one was synthesized by stirring a mixture of fluorescein isothiocyanate (350 mg) and *p*-aminobenzoic acid (137 mg) in dimethylformamide (3 mL) for 2 h at room temperature. The solvent was then removed by vacuum rotary evaporation at 60 °C. The residual oil was treated with chloroform until yellowish-orange crystals appeared. The yield was 571 mg. This was then mixed with dicyclohexylcarbodiimide (1.045 g) and *p*-guanidinobenzoic acid (1.093 g) in a 25-mL solution of equal parts of pyridine and dimethylformamide and stirred at room temperature for 16 h. The dicyclohexylurea was removed by filtration and the solvent mixture removed by rotary evaporation until all the dimethylformamide and pyridine was removed. Chloroform (250 mL) was then added and the mixture stirred until the oil solidified. The solid was resuspended in chloroform (250 mL) and the suspension stirred vigorously for 2 h at room temperature. The solid was removed by filtration and resuspended in chloroform, and the cycle was repeated. Finally, the solid was filtered and dried in vacuo at room temperature. The product (1.265 g) appeared as a pale, yellow powder. When stored at 4 °C under vacuum, the crude derivative is stable for at least 1 year. The structures of FDE and FME are being confirmed by chemical methods.

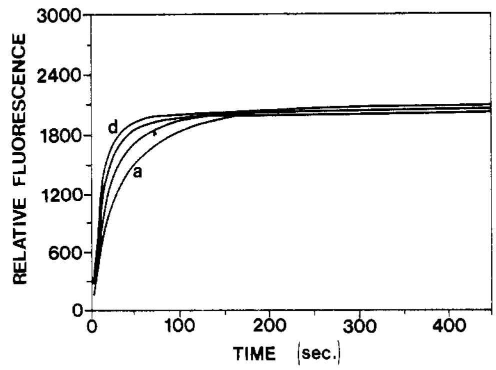

FIGURE 2: Kinetics of hydrolysis of increasing concentrations of FDE by trypsin. Solutions of phosphate-buffered saline containing 1.07 $\times 10^{-7}$ M trypsin and 3 $\times 10^{-5}$ M benzamidine were incubated with FDE at concentrations of (a) 5.40 $\times 10^{-7}$ M, (b) 8.09 $\times 10^{-7}$ M, (c) 1.09 $\times 10^{-6}$ M, and (d) 1.46 $\times 10^{-6}$ M, and the increase in fluorescence was monitored as a function of time (see Materials and Methods).

A recent preparation of FDE was shown to be 99.2% fluorogenically pure; i.e., the magnitude of the fluorescence of a solution of FDE in phosphate-buffered saline was 0.8% of the fluorescence from the same amount of FDE which had been hydrolized by alkali and measured in phosphate-buffered saline.

Kinetics of Hydrolysis of FDE by Trypsin. The acyl-enzyme theory was developed by Bender et al. (1967) to describe the kinetics of hydrolysis of certain amide and ester bonds by serine proteases. If FDE is an active-site titrant of trypsin, then, according to this theory, the hydrolysis of FDE by the esterase activity of trypsin should proceed by the three-step mechanism

$$E + S \overset{K_s}{\rightleftharpoons} E\cdot S \xrightarrow{k_2} ES' + P_1 \xrightarrow{k_3} E + P_2 \quad (1)$$

where E is trypsin, S is FDE, E·S is the adsorptive enzyme–substrate complex, ES′ is the covalent acyl-enzyme intermediate, *p*-guanidinobenzoyl-trypsin, P_1 is FME, P_2, the other product of the reaction, is *p*-guanidinobenzoate, K_s is the equilibrium dissociation constant, k_2 is the first-order acylation rate constant, and k_3 is the first-order deacylation rate constant.

The kinetics of hydrolysis of different concentrations of FDE by trypsin are shown in Figure 2. Benzamidine, a competitive inhibitor, was present so that the substrate dependence of the rate of the reaction could more easily be observed. The reaction, when monitored by the appearance of P_1, appears biphasic. There is an initial "burst" of P_1, followed by a very slow linear increase. The initial burst or pre-steady-state phase is due to the rapid formation of the covalent acyl-enzyme intermediate, *p*-guanidinobenzoyl-trypsin, and the concomitant release of a stoichiometric amount of the highly fluorescent FME. Thereafter, the "postburst" or steady-state phase is reached, during which deacylation of the enzyme occurs very slowly.

A mathematical solution of the reaction sequence in eq 1 which describes the appearance of P_1 as a function of time and substrate concentration is

$$[P_1] = At + B(1 - e^{-bt}) \quad (2)$$

where

$$A = \frac{k_{cat}[E]_0[S]_0}{[S]_0 + K_{m(app)}} \quad (3)$$

$$B = [E]_0\left[\frac{(k_{cat}/k_3)[S]_0}{[S]_0 + K_{m(app)}}\right]^2 \quad (4)$$

$$b = \frac{(k_2 + k_3)[S]_0 + k_3K_s}{K_s + [S]_0} \quad (5)$$

$$k_{cat} = \frac{k_2k_3}{k_2 + k_3} \quad (6)$$

$$K_{m(app)} = \frac{K_sk_3}{k_2 + k_3} \quad (7)$$

Equation 2 describes the form of the titration curves in Figure 2a. At t approaching infinity, $[P_1] = At + B$, the straight line of the steady-state portion of the curves. At t approaching zero, $[P_1] = At + B - Be^{-bt}$, the "burst" or pre-steady-state portion of the curves.

The kinetic profiles in Figure 2 imply that the hydrolysis of FDE by trypsin proceeds by the reaction sequence shown in eq 1 and that FDE is a good active-site titrant of trypsin. At constant enzyme concentration, the rate of formation of P_1 during the pre-steady-state phase increases with increasing substrate concentration, while the rate of formation of P_1 during the steady-state phase is independent of substrate concentration. For a substrate to be deemed a good active-site titrant, not only must the burst be first order in substrate and the steady-state zero order in substrate but also the magnitude of the "burst" must be equivalent to the molar concentration of active sites. This is theoretically valid only if $k_2 \gg k_3$ and if the substrate concentration is much greater than the $K_{m(app)}$. If these two criteria are fulfilled in an active-site titration, extrapolation of the steady-state line to the ordinate will yield the enzyme concentration.

Determination of the Microscopic Rate Constants for FDE and NPGB with Trypsin. The pre-steady-state phase of an active-site titration of trypsin with either FDE or NPGB is too rapid to monitor with ordinary instrumentation. A competitive inhibitor can be used to slow the rate of the reaction. With the assumption that $k_2 \gg k_3$ and $[S]_0 \gg K_{m(app)}$ and with the presence of a competitive inhibitor (I), eq 5 can be reduced and rearranged to

$$\frac{1}{b} = \frac{K_s}{k_2K_I[S]_0}[I] + \frac{K_s + [S]_0}{k_2[S]_0} \quad (8)$$

For determination of K_I, k_2, and K_s for the reaction of FDE with trypsin, the kinetics of hydrolysis of four different concentrations of FDE by a 9 $\times 10^{-9}$ M solution of trypsin were monitored (see Materials and Methods) in the presence of the competitive inhibitor benzamidine. The values of b were calculated and plotted as $1/b$ vs. [I] (Figure 3A). The four lines from the four different FDE concentrations intersect to give a K_I of 1.82 $\times 10^{-5}$ M and a k_2 of 1.05 s^{-1}. From the slopes of the four lines, K_s was calculated to be 3.06 $\times 10^{-6}$ M.

For determination of k_2 and K_s for the reaction of NPGB with trypsin, the kinetics of hydrolysis of NPGB by a 1.82 $\times$ 10^{-6} M solution of trypsin were monitored (see Materials and Methods) in the presence of benzamidine. The values of b were then calculated (see Materials and Methods) and plotted as $1/b$ vs. [I] (Figure 3B). By use of the value for K_I determined above, the slope and the intercept yield k_2 = 0.370 s^{-1} and K_s = 1.49 $\times 10^{-7}$ M.

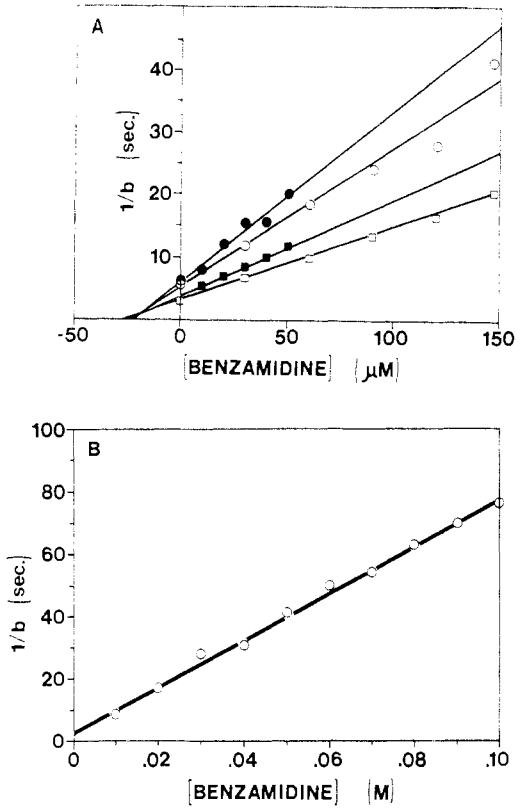

FIGURE 3: Determination of the microscopic kinetic constants K_s and k_2 for the hydrolysis by trypsin of (A) FDE and (B) NPGB. (A) The kinetics of hydrolysis of four different concentrations of FDE in phosphate-buffered saline containing 9×10^{-9} M trypsin and the indicated concentrations of benzamidine were monitored (data not shown), and the first-order rate constant b for each inhibitor concentration was determined (see Materials and Methods). The FDE concentrations were (●) 6.8×10^{-7} M, (○) 7.6×10^{-7} M, (■) 9.7×10^{-7} M, and (□) 1.1×10^{-6} M. (B) The kinetics of hydrolysis of a 2.96×10^{-5} M solution of NPGB in phosphate-buffered saline containing 1.82×10^{-6} M trypsin and the indicated concentrations of benzamidine were monitored (data not shown), and the first-order rate constant, b, for each inhibitor concentration was determined (see Materials and Methods.

The first-order rate constant for deacylation, k_3, is defined according to eq 1:

$$\ln \frac{[ES']_t}{[ES']_0} = -k_3 t \qquad (9)$$

where $[ES']_t$ is the concentration of acylated enzyme at time t, $[ES']_0$ is the concentration of acylated enzyme at time zero, and $[ES']_t = [ES']_0 - [E]_t$, where $[E]_t$ is the concentration of deacylated enzyme at time t. Normally the rate of deacylation is determined by incubating enzyme with titrant, separating unreacted titrant from acylated enzyme by exclusion column chromatography, and monitoring the return of active enzyme as a function of time. A major difficulty with this method is in determining $[ES']_0$ after column chromatography. Since the same acyl-enzyme intermediate is formed when trypsin reacts with either FDE or NPGB, exclusion column chromatography can be avoided. Instead, an aliquot of NPGB sufficient to acylate about 90% of the enzyme is added to a solution of trypsin whose molar concentration is known. An aliquot of that solution is then titrated with FDE to determine $[ES']_0$. The rate of deacylation is then determined by titrating aliquots of the solution with FDE after various time intervals to measure the increase in the amount of free enzyme. The results are shown in Figure 4. The first-order rate constant, k_3, for the deacylation of *p*-guanidinobenzoyl-trypsin is 1.66×10^{-5} s^{-1}.

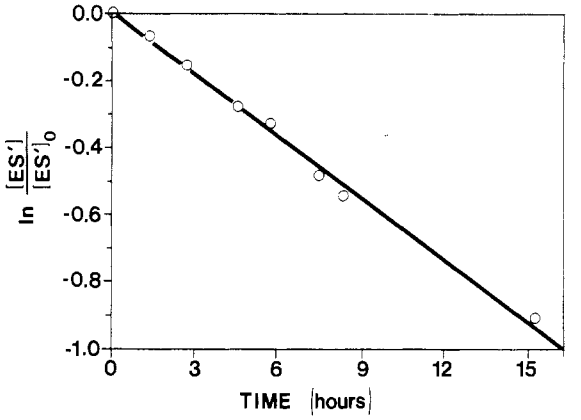

FIGURE 4: Determination of the first-order rate constant, k_3, for the deacylation of *p*-guanidinobenzoyl-trypsin. At zero time, NPGB to a concentration of 2.9×10^{-5} M is added to a 2.87×10^{-5} M solution of trypsin in phosphate-buffered saline. Five minutes later, benzamidine is added to a concentration of 9.8×10^{-4} M. The concentration of acylated enzyme was then determined by an active-site titration with FDE of an aliquot of the solution. The result indicated that the concentration of acylated enzyme was 2.50×10^{-5} M. At the indicated times, an aliquot of the reaction mixture was withdrawn, and the amount of deacylated enzyme was determined by an active-site titration with FDE.

From this kinetic analysis, FDE has been shown to be an excellent active-site titrant of trypsin. Both major assumptions used in the derivation of the kinetic constants, $k_2 \gg k_3$ and $[S]_0 \gg K_{m(app)}$, are valid. The $K_{m(app)}$, calculated by using eq 7, is 4.85×10^{-11} M for FDE and trypsin and 6.66×10^{-12} for NPGB and trypsin. Under conditions in which the major assumptions are valid, the value of B in eq 4 equals $[E]_0$. Thus, the steady-state line, eq 2 at t approaching infinity, now reduces to $[P_1] = k_{cat}[E]_0 t + [E]_0$, so that extrapolation of the steady-state line to zero time yields $[E]_0$. For measurement of the concentration of active sites in a solution of trypsin, all that is needed is to determine the magnitude of the fluorescent "burst". The steady-state line has such a small slope that extrapolation to time zero is not necessary. The molar concentration of a solution of FME which exhibits the same amount of fluorescence is then equal to the molar concentration of active sites in the solution of trypsin. This is shown in Figure 5 where increasing concentrations of trypsin are titrated (Figure 5A) and the "burst" values plotted vs. the trypsin concentration (Figure 5B).

Properties of FDE and Its Derivatives. When FDE is hydrolyzed by alkali, the product is 5-[*N'*-(4-carboxyphenyl)-thioureido]-3',6'-dihydroxyspiro[isobenzofuran-1(3*H*),9'-[9*H*]xanthen]-3-one (FUE, fluorescein unesterified) (Figure 1C). The excitation maximum of FUE in phosphate-buffered saline is 491 nm, and the emission maximum is 514 nm. The relative quantum yield of FUE in phosphate-buffered saline is 0.64, using 0.92, the quantum yield of fluorescein, as the standard. This relative quantum yield remains constant when measured in solutions of phosphate-buffered saline whose pH ranges from 7.0 to 12.0. The lifetime of the excited state of FUE in phosphate-buffered saline is 4.4 ns when determined by phase and 4.1 ns when determined by modulation. Under similar conditions, the lifetime of the excited state of fluorescein is 4.5 ns when determined by phase and 4.2 ns when determined by modulation. The absorption and emission spectra of FUE as well as its quantum yield and the lifetime of the excited state are identical with those exhibited by the product of an active-site titration of trypsin by FDE.

FDE is relatively stable in aqueous buffers. However, ester bonds do spontaneously hydrolyze in aqueous solutions at rates

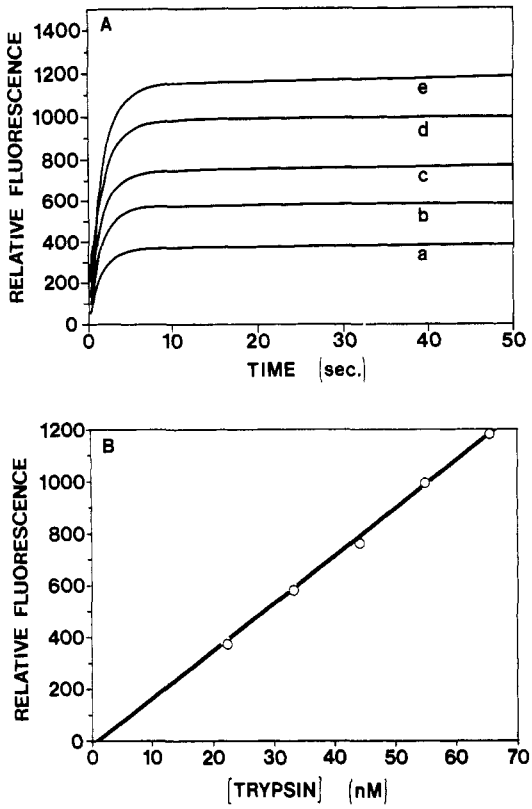

FIGURE 5: Hydrolysis of FDE as a function of the trypsin concentration. (A) Solutions of phosphate-buffered saline containing 4.30 × 10^{-6} M FDE were incubated with trypsin at concentrations of (a) 2.23 × 10^{-8} M, (b) 3.32 × 10^{-8} M, (c) 4.41 × 10^{-8} M, (d) 5.49 × 10^{-8} M, and (e) 6.55 × 10^{-8} M, and the increase in fluorescence was monitored as a function of time (see Materials and Methods). (B) The magnitude of the fluorescent plateau, at 120 s, for the five curves in (A) are plotted vs. the trypsin concentration. The trypsin concentrations were determined by an NPGB active-site titration.

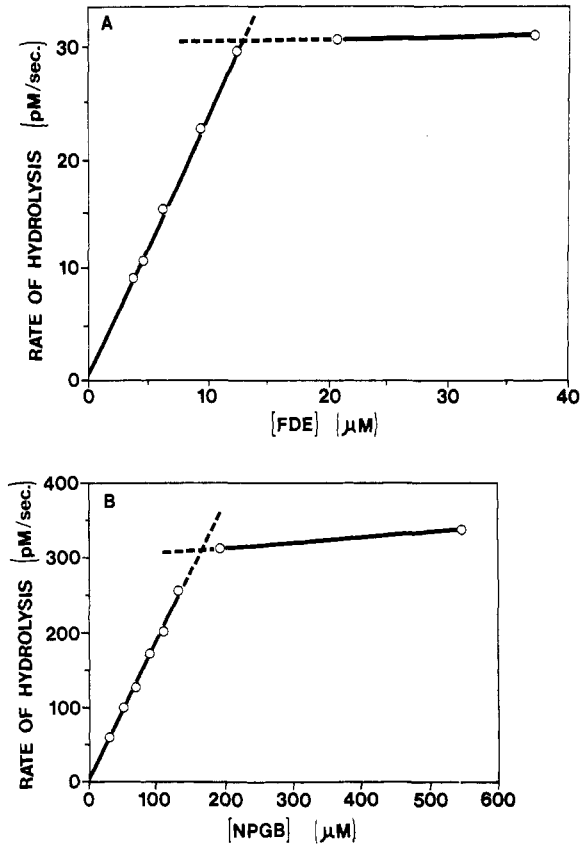

FIGURE 6: Determination of the first-order rate constant for spontaneous hydrolysis and determination of the solubility limit of (A) FDE and of (B) NPGB in phosphate-buffered saline. (A) Aliquots from a 7.3 × 10^{-3} M solution of FDE in dimethylformamide were added to solutions of phosphate-buffered saline. Each solution of FDE in phosphate-buffered saline was then centrifuged for 2 min at 8000*g* to remove any precipitate. The rate of spontaneous hydrolysis of FDE, d(F)/d*t*, was determined by measuring the increase in fluorescence over a 30-min period. This rate is plotted vs. the amount of FDE added to phosphate-buffered saline. (B) Aliquots from a 2.72 × 10^{-2} M solution of NPGB in dimethylformamide were added to solutions of phosphate-buffered saline. Each solution of NPGB in phosphate-buffered saline was then centrifuged for 2 min at 8000g to remove any precipitate. The rate of spontaneous hydrolysis, d(OD)/d*t*, was determined by measuring the increase in optical density at 400 nm in a spectrophotometer over a 48- period. This rate is plotted vs. the amount of NPGB added to phosphate-buffered saline.

which are proportional to their concentration. The first-order rate constant for the spontaneous hydrolysis of FDE, $k_{(spont)}$, is defined as

$$\ln \frac{[FDE]_t}{[FDE]_0} = -k_{(spont)}t \qquad (10)$$

where $[FDE]_t$ is the concentration of FDE at time t and $[FDE]_0$ is the concentration of FDE at time zero. $[FDE]_t = [FDE]_0 - [FME]_t$ where $[FME]_t$ is the concentration of hydrolyzed FDE at time t. The first-order rate constant, $k_{(spont)}$, for spontaneous hydrolysis can be measured by incubating FDE in phosphate-buffered saline and monitoring the increase in fluorescence as a function of time. The first-order rate constant for spontaneous hydrolysis of FDE in phosphate-buffered saline is 5.1 × 10^{-6} s^{-1} (data not shown). Under identical conditions, the first-order rate constant for the spontaneous hydrolysis of NPGB is 2.0 × 10^{-6} s^{-1} (data not shown).

The solubility limit of FDE in phosphate-buffered saline can be determined indirectly. Since the rate of spontaneous hydrolysis is proportional to the concentration of FDE in solution (eq 11), a saturated solution can be defined as one in which the rate of spontaneous hydrolysis is independent of the addition of more FDE. For determination of the solubility limit, increasing amounts of FDE are added to solutions of phosphate-buffered saline, and the insoluble material is removed by centrifugation. The rate of spontaneous hydrolysis for each solution is then measured and plotted vs. the FDE concentration (Figure 6A). Saturation can be defined as the intersection of the two lines, i.e., where the rate of spontaneous hydrolysis becomes independent of the amount of FDE added. For FDE in phosphate-buffered saline at pH 7.2, saturation is 1.3 × 10^{-5} M. A saturated solution of NPGB under similar conditions is 1.7 × 10^{-4} M (Figure 6B).

Kinetics of Hydrolysis of FDE by Urokinase and Plasmin. Having demonstrated FDE is similar kinetically to NPGB in an active-site titration of trypsin and described some of the properties of FDE, we next asked if FDE is a good active-site titrant of other serine proteases. The kinetics of hydrolysis of FDE by urokinase and plasmin are shown in Figure 7. These kinetic profiles are similar to that observed with the hydrolysis of FDE by trypsin. Since urokinase and plasmin are serine proteases, the hydrolysis of FDE by their esterase activities (Lorand & Condit, 1965; Chase & Shaw, 1969) should proceed by way of an acyl-enzyme intermediate according to the reaction sequence in eq 1.

Determination of the Microscopic Rate Constants for FDE with Urokinase. For determination of k_2 and K_s for the reaction of FDE with urokinase, the kinetics of hydrolysis by a 1.11 × 10^{-7} M solution of urokinase were monitored (see Materials and Methods) at various FDE concentrations. The values of b were then determined and plotted as $1/b$ vs. $1/$

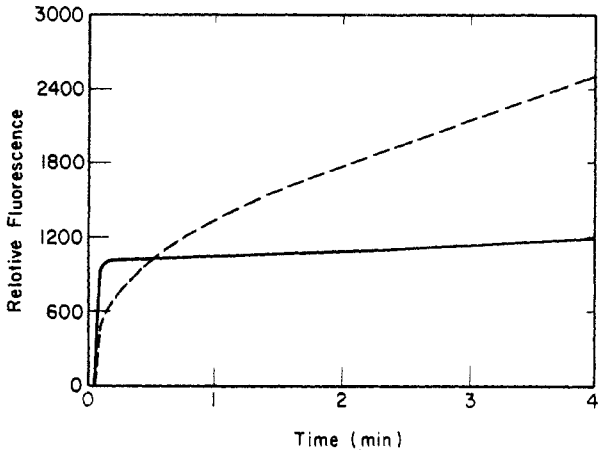

FIGURE 7: Kinetics of hydrolysis of FDE by urokinase (dashed line) and plasmin (solid line). A 1.0-mL solution of phosphate-buffered saline containing 8.0×10^{-6} M FDE and 44 Plough units of urokinase, 9.15×10^{-9} M as determined by an FDE active-site titration, was incubated at room temperature, and the kinetics of hydrolysis of FDE were monitored as described under Materials and Methods. A 1.0-mL solution of phosphate-buffered saline containing 1.6×10^{-6} M FDE and 8.99×10^{-9} M plasmin, whose concentration was determined by an FDE active-site titration, was incubated at room temperature, and the kinetics of hydrolysis of FDE were monitored.

[FDE] (Figure 8A). With the assumption that $k_2 \gg k_3$ and $[S]_0 \gg K_{m(app)}$, the following relationship can be derived from eq 5:

$$\frac{1}{b} = \frac{1}{k_2} + \frac{K_s}{k_2[S]_0} \quad (11)$$

The intercept in Figure 8A yields a k_2 of 0.112 s^{-1} and the slope a K_s of 2.71×10^{-5} M.

The first-order rate constant for the deacylation of *p*-guanidinobenzoyl-urokinase, k_3, can be determined by analysis of the slopes of the steady-state lines of the titration curves. The expression for the rate of "postburst" or steady-state production of P_1 is

$$\frac{d[P_1]}{dt} = \frac{k_{cat}[E]_0[S]_0}{K_{m(app)} + [S]_0} + k_{(spont)}[S]_0 + k_{nas}[E]_0[S]_0 \quad (12)$$

where the first term is the rate of active-site hydrolysis of FDE, the second term is the rate of spontaneous hydrolysis of FDE, and the third term is the rate of nonactive site induced hydrolysis of FDE. If $[S]_0 \gg K_{m(app)}$, eq 12 can be reduced and rearranged to

$$\frac{d[P_1]/dt}{[E]_0} = k_{pb} = \frac{k_{(spont)}}{[E]_0} + k_{nas}[S]_0 + k_{cat} \quad (13)$$

The "postburst" portion of a series of titration curves was analyzed and the data were plotted as k_{pb} vs. [FDE] (Figure 8B). The intercept yields a k_{cat} of 3.64×10^{-4} s^{-1}. Since $k_{cat} = k_2k_3/(k_2 + k_3)$ and since $k_2 \gg k_3$, then k_3 is approximately equal to k_{cat}. The $k_{(spont)}$ had been previously determined; hence, for this specific preparation of urokinase, k_{nas} is 261 M^{-1} s^{-1}.

Determination of the Microscopic Constants for FDE with Plasmin. The kinetics of hydrolysis of FDE by plasmin are too fast to monitor with ordinary instrumentation (Figure 7). For accurate measurement of the burst, the competitive inhibitor benzamidine was again used to slow the rate of the reaction. The relationship defined by eq 5 can then be used to determine K_I, k_2, and K_s. The kinetics of hydrolysis of two different concentrations of FDE by a 9×10^{-9} M solution of

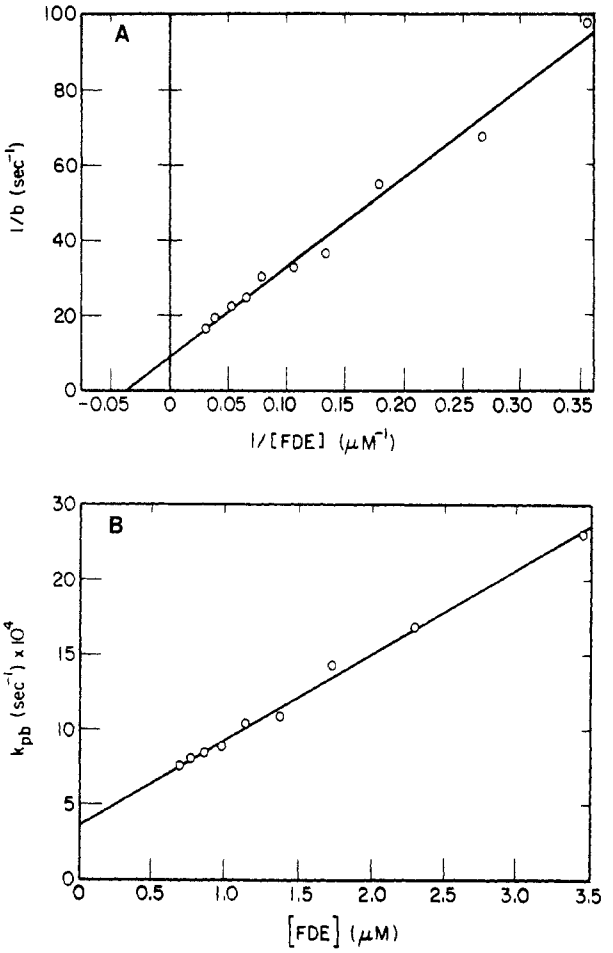

FIGURE 8: Determination of the microscopic kinetic constants for the hydrolysis of FDE by urokinase. (A) The kinetics of hydrolysis of the indicated concentrations of FDE in phosphate-buffered saline containing 9.93×10^{-8} M urokinase were monitored (data not shown). The first-order rate constant, *b*, for each FDE concentration was then calculated (see Materials and Methods), and its reciprocal is plotted vs. the reciprocal of the FDE concentration. (B) The steady-state kinetics of hydrolysis of the indicated concentrations of FDE by a 1.63×10^{-8} M solution of urokinase in phosphate-buffered saline were monitored (data not shown). The first-order rate constant, k_{pb}, for each FDE concentration was then calculated and plotted vs. the FDE concentration.

plasmin were monitored in the presence of various concentrations of the competitive inhibitor benzamidine (see Materials and Methods). The values of *b* were then calculated. A plot of $1/b$ vs. [I] yielded two straight lines which intersect to give a K_I of 1.87×10^{-4} M and a k_2 of 0.799 s^{-1} (Figure 9A). From the slopes of the two lines, K_s was calculated to be 6.04×10^{-6} M. The rate of deacylation of *p*-guanidinobenzoyl-plasmin was determined in a manner similar to that used to determine the rate of deacylation of *p*-guanidinobenzoyl-trypsin. The results are shown in Figure 9B. The first-order rate constant, k_3, for the deacylation of *p*-guanidinobenzoyl-plasmin is 6.27×10^{-6} s^{-1}.

Discussion

FDE was designed as an active-site titrant of serine proteases to exhibit the same excellent kinetic characteristics as NPGB and to liberate a product in an active-site titration as detectable as fluorescein. Kézdy & Kaiser (1970) have listed criteria which must be satisfied for a reagent to be a useful active-site titrant. These criteria are fulfilled by FDE: (1) The rate constants exhibited in an active-site titration of trypsin by FDE are comparable to those exhibited by NPGB, indicating that catalysis by the enzyme occurs. (2) Kinetic profiles of ac-

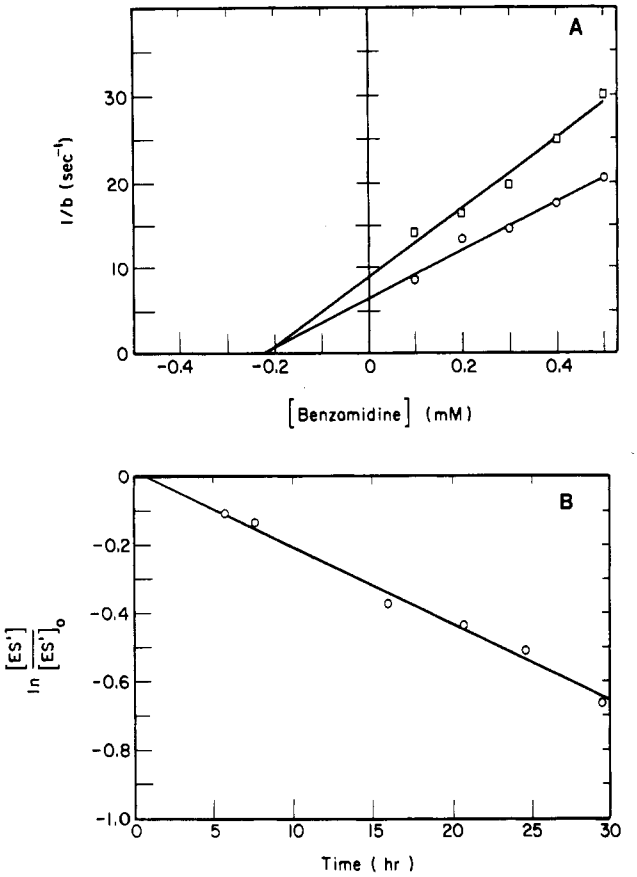

FIGURE 9: Determination of the microscopic kinetic constants for the hydrolysis of FDE by plasmin. (A) The kinetics of hydrolysis of two different concentrations of FDE in phosphate-buffered saline containing 1.10×10^{-8} M plasmin and the indicated concentrations of benzamidine were monitored (data not shown). The first-order rate constant, b, for each inhibitor concentration was then calculated (see Materials and Methods) and its reciprocal plotted vs. the benzamidine concentration. The FDE concentrations were 9.72×10^{-7} M (□) and 1.46×10^{-6} (○). (B) At time zero, NPGB is added to a final concentration of 10^{-5} M to a 1.31×10^{-5} M solution of plasmin in phosphate-buffered saline containing 0.02 M lysine. Five minutes later, benzamidine is added to a concentration of 0.001 M. The concentration of acylated enzyme was then determined by an active-site titration with FDE of an aliquot of the solution. The result showed the concentration of acylated enzyme was 1.07×10^{-5} M. At the times indicated on the abscissa, aliquots of the solution were withdrawn, and the amount of deacylated enzyme was determined by an active-site titration with FDE.

tive-site titrations show that the "burst" is first order in substrate and the steady state is zero order in substrate, indicating the titrations obey acyl-enzyme kinetic theory. (3) Benzamidine is a competitive inhibitor in an active-site titration of trypsin with FDE, implying that FDE binds to the active site. (4) One molecule of FDE reacts with one molecule of trypsin, resulting in the formation of an inactive intermediate. This is the predicted stoichiometry of an irreversible reaction resulting in an acyl-enzyme product. (5) Eventually full enzymatic activity is restored, implying deacylation has occurred.

FDE and NPGB exhibit similar excellent kinetic constants in an active-site titration of trypsin (Table I). The kinetic parameters which are indicative of the usefulness of a compound as an active-site titrant are k_2, k_3, and $K_{m(app)}$. The acylation rate constant, k_2, is slightly larger for FDE than for NPGB, allowing for a more rapid completion of the pre-steady-state phase of a titration. The deacylation rate constant, k_3, is the same for both titrants and is so low that little turnover occurs. The $K_{m(app)}$ for NPGB is approximately 7-fold lower than that for FDE, although the values for both are extremely

Table I: Characteristics of FDE and NPGB

	FDE-trypsin	NPGB-trypsin	FDE-urokinase	FDE-plasmin
1. Kinetic Constants				
k_2 (s^{-1})	1.05	0.370	0.112	0.799
k_3 (s^{-1})	1.66×10^{-5}	1.66×10^{-5}	3.64×10^{-4}	6.27×10^{-6}
K_s (M)	3.06×10^{-6}	1.49×10^{-7}	2.71×10^{-5}	6.04×10^{-6}
$K_{m(app)}$ (M)	4.85×10^{-11}	6.66×10^{-12}	8.78×10^{-8}	4.74×10^{-11}
k_2/K_s (M^{-1} s^{-1})	3.48×10^{5}	2.45×10^{6}	4.13×10^{3}	1.28×10^{5}

	FDE	NPGB
2. Other Parameters		
$k_{(spont)}$ (s^{-1})	5.1×10^{-6}	2.0×10^{-6}
saturation (M)	1.3×10^{-5}	1.7×10^{-4}

small. Since a saturated solution of FDE in phosphate-buffered saline is 1.3×10^{-5} M, titrations can easily be performed under conditions in which $[S]_0 \gg K_{m(app)}$. The difference in $K_{m(app)}$ values is primarily a reflection of the lower K_s exhibited by NPGB. An obvious explanation for this difference in the equilibrium dissociation constants is that formation of the adsorptive enzyme–substrate complex is sterically hindered to a greater extent by the larger xanthene ring of FDE than it is by the much smaller p-nitrophenol ring of NPGB.

An important kinetic characteristic of both FDE and NPGB is the very slow rate of deacylation. p-Guanidinobenzoyl-trypsin exhibits a half-time for deacylation in phosphate-buffered saline of 12 h. Thus the slope of the steady-state line of a titration curve is small, allowing for easy extrapolation to zero time to obtain the enzyme concentration. A small k_3 also results in a low $K_{m(app)}$ and a high k_2/k_3 ratio so that the size of the burst is not affected by the substrate concentration under most titration conditions. The structural basis for the difficulty in deacylation is not apparent.

The major difference between FDE and NPGB is the detectability of the product in an active-site titration. At pH 7.2, fluorescein can be detected at concentrations as low as 10^{-12} M whereas p-nitrophenol can be detected at concentrations no lower than 10^{-6} M. Even without taking advantage of the sensitivity of fluorescence, the product of an active-site titration with FDE is more detectable spectrophotometrically than with NPGB because FME has a larger extinction coefficient than p-nitrophenol. Another advantage of FDE is that active-site titrations can be performed at pH 7.2 whereas titrations with NPGB should be performed at pH 8.3 where p-nitrophenol is greater than 90% ionized, thereby nearly exhibiting its maximum extinction coefficient (Chase & Shaw, 1970). Titrations at physiologic pH are obviously advantageous for certain serine proteases. Also, the rate of spontaneous hydrolysis of both FDE and NPGB is much less at pH 7.2 than pH 8.3. At pH 8.3, the rate of spontaneous hydrolysis of FDE is 5-fold greater than that at pH 7.2 whereas with NPGB the rates differ by 10-fold.[2]

Heretofore, the most sensitive active-site titrants for serine proteases have been the coumarin derivatives, e.g., the 4-methylumbelliferyl ester of p-guanidinobenzoate (Jameson et al., 1973). FUE has an extinction coefficient 5-fold greater than umbelliferone, has a quantum yield at least twice as great, and absorbs maximally at 491 nm where the xenon lamp output is twice that at 325 nm, the absorption maximum for 4-methyl-7-hydroxycoumarin. Furthermore, in selecting

[2] J. F. Cannon and W. F. Mangel, unpublished observations.

wavelengths that optimize the difference in fluorescence between the coumarin substrate and its hydrolysis product, only 22% of the maximal fluorescence is retained (Zimmerman et al., 1977). Thus, the detectability of the product of an active-site titration with FDE is much greater than that with the coumarin derivatives. Also, fluorescein is completely colorless and nonfluorescent in the lactone state whereas the derivatives of coumarin exhibit intrinsic fluorescence.

FDE is also useful as an active-site titrant of other serine proteases, as demonstrated by the characterization of its interaction with two of the enzymes involved in fibrinolysis. The rate of acylation of both urokinase and plasmin by FDE is much greater than their rates of deacylation (Table I). The $K_{m(app)}$ of FDE for both enzymes is extremely low, thereby allowing the molar concentration of active sites to be determined easily from a single titration. The rapid rate of acylation and high extinction coefficient and quantum yield of the product of an active-site titration are particularly advantageous. This allows these proteases to be assayed at low concentrations where the rate of self-proteolysis is negligible. This characteristic of FDE is exploited in the following paper in this issue (Leytus et al., 1981) in which the activation of plasminogen by a transformed cell-associated plasminogen activator and by urokinase is quantitatively characterized.

Acknowledgments

We thank Dr. G. Weber and the members of his laboratory, in particular R. Hall, D. M. Jameson, R. B. Macgregor, and P. M. Torgerson, for their help in measuring fluorescent lifetimes and quantum yields.

References

Beers, W. H., Strickland, S., & Reich, E. (1975) *Cell (Cambridge, Mass.) 6*, 387–394.

Bender, M. L., Begué-Canton, M. L., Blakley, R. L., Brubacher, L. J., Feder, J., Gunter, C. R., Kézdy, F. J., Killhefter, J. V., Jr., Marshall, T. H., Miller, C. G., Roeske, R. W., & Stoops, J. K. (1966) *J. Am. Chem. Soc. 88*, 5890–5913.

Bender, M. L., Kézdy, F. J., & Wedler, F. C. (1967) *J. Chem. Educ. 44*, 84–88.

Castellino, F. J., & Sodetz, J. M. (1976) *Methods Enzymol. 45*, 273–286.

Chase, T., & Shaw, E. (1967) *Biochem. Biophys. Res. Commun. 29*, 508–514.

Chase, T., & Shaw, E. (1969) *Biochemistry 8*, 2212–2224.

Chase, T., & Shaw, E. (1970) *Methods Enzymol. 19*, 20–27.

Christman, J. K., Selgi, S., Newcomb, E. W., Silverstein, S. C., & Acs, G. (1975) *Proc. Natl. Acad. Sci. U.S.A. 72*, 47–50.

Jameson, G. W., Roberts, D. V., Adams, R. W., Kyle, W. S. A., & Elmore, D. T. (1973) *Biochem. J. 131*, 107–117.

Jameson, D. M., Williams, J. F., & Wehrly, J. A. (1977) *Anal. Biochem. 79*, 623–626.

Jones, P. A., Laug, W. E., & Benedict, W. F. (1975) *Cell (Cambridge, Mass.) 6*, 245–252.

Kézdy, F. J., & Kaiser, E. T. (1970) *Methods Enzymol. 19*, 3–19.

Leytus, S. P., Cannon, J. F., Peltz, G. A., Liu, H.-Y., Peltz, S. W., Livingston, D. C., Brocklehurst, J. R., & Mangel, W. F. (1981) *Biochemistry* (following paper in this issue).

Liu, H.-Y., Peltz, G. A., Leytus, S. P., Livingston, C., Brocklehurst, J., & Mangel, W. F. (1980) *Proc. Natl. Acad. Sci. U.S.A. 77*, 3796–3800.

Lorand, L., & Condit, E. V. (1965) *Biochemistry 4*, 265–270.

Miskin, R., & Reich, E. (1980) *Cell (Cambridge, Mass.) 19*, 217–224.

Ossowski, L., Quigley, J. P., Kellerman, G. M., & Reich, E. (1973a) *J. Exp. Med. 138*, 1056–1064.

Ossowski, L., Unkeless, J. C., Tobia, A., Quigley, J. P., Rifkin, D. B., & Reich, E. (1973b) *J. Exp. Med. 137*, 112–126.

Ossowski, L., Quigley, J. P., & Reich, E. (1975) *Cold Spring Harbor Conf. Cell Proliferation 2*, 901–913.

Parker, C. A., & Rees, W. T. (1960) *Analyst 85*, 587–600.

Pollack, R., Risser, R., Canlon, S., & Rifkin, D. (1974) *Proc. Natl. Acad. Sci. U.S.A. 71*, 4792–4796.

Reich, E., Rifkin, D. B., & Shaw, E. (1975) *Cold Spring Harbor Conf. Cell Proliferation 2*, 1–987.

Seybold, P. G., Gouterman, M., & Callis, J. (1969) *Photochem. Photobiol. 9*, 229–242.

Spencer, R. D., & Weber, G. (1969) *Ann. N.Y. Acad. Sci. 158*, 361–376.

Strickland, S., Reich, E.,, & Sherman, M. I. (1976) *Cell (Cambridge, Mass.) 9*, 231–240.

Unkeless, J. C., Tobia, A., Ossowski, L., Quigley, J. P., Rifkin, D. B., & Reich, E. (1973) *J. Exp. Med. 137*, 85–111.

Weber, G., & Teale, F. W. J. (1957) *Trans. Faraday Soc. 53*, 646–655.

Wehrly, J. A. (1979) Ph.D. Thesis, University of Illinois, Urbana, IL.

Wehrly, J. A., Williams, J. F., Jameson, D. M., & Kolb, D. A. (1976) *Anal. Chem. 48*, 1424–1426.

Zimmerman, M., Ashe, B., Yurewicz, E. C., & Patel, G. (1977) *Anal. Biochem. 78*, 47–51.